doi.org/10.36721/PJPS.2026.39.9.244.1

Integration of network pharmacology, molecular docking and molecular dynamics simulation to explore active ingredients and mechanism of *sparganii rhizoma* on lung cancer

Wei Chang[1,4]*, Bingxuan Niu[2], Xuxu Yan[2] and Chenyang Hu[3,4]

[1]General Surgery Second Word, Xinxiang No.1 People's Hospital, Xinxiang 453700, Henan Province, PR China
[2]School of Pharmacy, Henan Medical University, Xinxiang 453002, Henan Province, PR China
[3]Respiratory and Critical Care Medical Department No.3 Word, Xinxiang No.1 People's Hospital, Xinxiang 453700, Henan Province, PR China
[4]The Affiliated People's Hospital of Henan Medical University, Xinxiang 453700, Henan Province, PR China

Abstract: **Background**: With high incidence and mortality rates, lung cancer has brought a huge burden to patients' families and society. *Sparganii Rhizoma*, a famous anti-cancer herb, has demonstrated good effects on lung cancer. However, the underlying active ingredients and mechanism of *Sparganii Rhizoma* on lung cancer were not yet clear. **Objectives**: This study integrated network pharmacology, molecular docking and molecular dynamics simulation to explore the active ingredients and mechanism of *Sparganii Rhizoma* on Lung Cancer. **Methods**: Three databases and several related studies were used to screen the ingredients and targets of *Sparganii Rhizoma* and lung cancer, respectively. The enrichment analyses were performed using the Matascape database, and the protein-protein interaction (PPI) and ingredient-target-pathway networks were constructed. Finally, molecular docking and molecular dynamics simulations were used to verify the key active ingredients and targets of *Sparganii Rhizoma* in lung cancer. **Results**: A total of 129 ingredients and 1101 targets of *Sparganii Rhizoma*, and 150 targets of lung cancer, were obtained. Network pharmacology identified 57 active ingredients, 27 targets, and 86 signaling pathways for *Sparganii Rhizoma* in lung cancer. The results of molecular docking indicated that the key active ingredients included sparstolonin B, emodin, adenosine, 4-hydroxycinnamic acid, and so on, and the key targets were Cytochrome P450 1A2 (CYP1A2), Prostaglandin G/H synthase 2 (PTGS2), and Dual specificity mitogen-activated protein kinase kinase 1 (MAP2K1). In a molecular dynamics simulation, sparstolonin B bound to CYP1A2, PTGS2, and MAP2K1 with good affinity. **Conclusion**: Based on the integration of network pharmacology, molecular docking and molecular dynamics simulation, this study revealed the potential active ingredients and mechanisms of *Sparganii Rhizoma* on lung cancer.

Keywords: Lung cancer; Molecular docking; Molecular dynamics simulation; Network pharmacology; *Sparganii Rhizoma*

Submitted on 02-02-2026 – Revised on 28-02-2026 – Accepted on 04-03-2026

INTRODUCTION

Due to tobacco use, air pollution, and other risk pathogenic factors, lung cancer has become increasingly widespread globally. According to global cancer statistics released by the International Agency for Research on Cancer (IARC), lung cancer causes more than two million new cases and 1.8 million deaths per year (Filho *et al.*, 2025; Thai *et al.*, 2021; Nooreldeen and Bach, 2021). Lung cancer has been the most commonly diagnosed cancer and the leading cancer death for males and the second most frequent cancer for females (Filho *et al.*, 2025). In Eastern Asia, lung cancer has consistently ranked first in cancer deaths for a decade (Lee and Kazerooni, 2022; Detterbeck *et al.*, 2024). In China, there were an estimated 1.06 million new cases of lung cancer in 2022, which accounted for 22% of national cancer incidence and 40% of global cases. Furthermore, it was estimated that the The global cancer burden would double by 2050, so it would bring a huge disease burden to patients' families and society (Nooreldeen and Bach, 2021).

With a bad prognosis and a high mortality rate, the main treatment methods for lung cancer include surgery, immunotherapy, radiotherapy, chemotherapy, targeted therapy, and so on. However, these methods had many shortcomings, such as severe side effects, drug resistance and high costs. Unfortunately, the 5-year survival rate of lung cancer was less than 19% (Dai *et al.*, 2021). Therefore, there was an urgent need to explore new treatment methods and drugs for lung cancer. Based on the current knowledge, traditional medicines may be a promising and cost-effective therapy for lung cancer.

With a long history spanning more than 2,000 years and extensive clinical practice, traditional Chinese medicine has received increasing attention for its multiple bioactive ingredients, targets, and pathways in the treatment and management of lung cancer (Zhao *et al.*, 2023; Zhang *et al.*, 2024). Modern pharmacological research has

**Corresponding author:* e-mail: 15503739671m@sina.cn

demonstrated that traditional Chinese medicine was a promising complementary therapy for lung cancer (Xi *et al.*, 2025). A meta-analysis (N = 1,574; six medical databases) revealed that combining Shenfu Injection with platinum-based chemotherapy benefits patients with non-small-cell lung cancer by improving tumor response, Karnofsky performance score, and immune function, and reducing chemotherapy toxicity (Cao *et al.*, 2017). A randomized controlled trial involving 64 patients demonstrated that the traditional Chinese medicine treatment (Cinobufacini, herbal decoction and Chinese acupoint application) could improve quality of life, increase one-year survival rate and have similar effects on overall survival compared to maintenance chemotherapy (treated with pemetrexed) for lung cancer (Jiang *et al.*, 2016). Shen Ming *et al*. found that the polysaccharide from Astragalus membranaceus could inhibit the premetastatic niche and the recruitment of myeloid-derived suppressor cells in lung cancer (Shen *et al.*, 2023).

Due to the multiple ingredients and multiple targets in traditional Chinese medicine, it was very difficult to explore its bioactive ingredients and mechanisms, which also greatly limited its international application and in-depth development (Dai *et al.*, 2021). The emergence of network pharmacology, molecular docking and molecular dynamics simulation has provided a novel methodological perspective for the above problem.

Network pharmacology is a pharmacological approach that integrates systems biology, computational modeling and network analysis (Zhao *et al.*, 2023; Zhang *et al.*, 2024). It was very similar to the holistic, systematic, and comprehensive perspective of traditional Chinese medicine (Zhao *et al.*, 2023; Zhou *et al.*, 2022). So, it could study the relationships among herbs, ingredients, targets, and diseases from a network perspective. Based on silico structure - based method, molecular docking and molecular dynamics simulation could evaluate the binding site, the types of binding interaction and interaction force between ligand (active ingredient) and receptor (target), so they would offer an insightful perspective and comprehension for the molecular mechanism (Ye *et al.*, 2021; Liu *et al.*, 2024). In the present day, a considerable number of studies have been carried out to explore the active ingredients and mechanism of traditional Chinese medicine through network pharmacology, molecular docking and molecular dynamics simulation (Bisht *et al.*, 2024; Sun *et al.*, 2023; Luo *et al.*, 2023; Ye *et al.*, 2021; Liu *et al.*, 2024; Li *et al.*, 2023). Wuai Zhou *et al*. used network pharmacology to study the mechanism of Moluodan in chronic atrophic gastritis and found that Moluodan could promote apoptosis, regulate immune and metabolic functions and so on (Zhou *et al.*, 2022). Integrated with network pharmacology, molecular docking and molecular dynamics simulation, Amisha Bisht *et al* elucidated four crucial active ingredients, ten key targets and three pathways for the anti-aging activity of *tinospora cordifolia* (Bisht *et al.*, 2024); Sun Zhicheng *et al* elucidated MAPK3 as the key target of polydatin on spinal cord ischemia-reperfusion injury (Sun *et al.*, 2023); Liu Minglu discovered four active ingredients and the target - TP53 for Chufeng Qingpi decoction in the therapeutic management of schistosomiasis (Liu *et al.*, 2024).

Sparganii Rhizoma, known as *Sanleng* in Chinese, is the dry tuberous rhizome of *Sparganium stoloniferum* Buch. - Ham. (Sparganium genus, Sparganiaceae family). *Sparganii Rhizoma* was first recorded in *Herbal Supplements* (in Chinese: Ben Cao Shi Yi) from the Tang Dynasty (AD 618-907). As a perennial aquatic and marsh herb, it is mainly distributed in East Asia, Europe and Africa. In China, the primary production areas are located in Heilongjiang, Jilin, Henan, and other provinces (Jia *et al.*, 2021). In traditional Chinese medicine, it has a bitter and pungent flavor and a neutral property, and it has the effects of eliminating blood stasis, promoting Qi flow and relieving swelling and pain (Jia *et al.*, 2021). Modern pharmacological research has shown that the active ingredients of *Sparganii Rhizoma* include linear-diarylheptanoids, phenylpropanoids, flavonoids and others (Wei *et al.*, 2022; Jia *et al.*, 2021; Chang *et al.*, 2020) and it had the effect of anti-tumor, anti-thrombotic, analgesic, anti-inflammatory and so on (Zheng *et al.*, 2025; Wei *et al.*, 2022; Jia *et al.*, 2021; Chang *et al.*, 2020; Liu *et al.*, 2023). In recent years, increasing attention has focused on its potential anticancer effects (Jia *et al.*, 2021; Wei *et al.*, 2022; Zheng *et al.*, 2025; Detterbeck *et al.*, 2024; Chang *et al.*, 2020; Dai *et al.*, 2021). Dai et al. found that the herbal combination of Sparganii Rhizoma and Curcumae had a good effect on lung cancer by upregulating mitochondrial-mediated caspase-dependent apoptosis signaling in human lung adenocarcinoma H1975 cells (Dai *et al.*, 2021). Research by Liu Jing et al. has shown that Sparganii Rhizoma can significantly improve lung function, slow the progression of lung tissue lesions and reduce collagen deposition (Liu *et al.*, 2023).

As a famous anti-cancer herb for years, the underlying active ingredients and mechanism of *Sparganii Rhizoma* on lung cancer have not yet been clear. Based on the integration of network pharmacology, molecular docking, and molecular dynamics simulation, this study aimed to identify potential active ingredients and the mechanism of Sparganii Rhizoma in lung cancer. A comprehensive network of active ingredients, targets, and signaling pathways, along with the PPI network, was constructed to investigate these components. The GO and KEGG enrichment analyses were performed to study the biological mechanisms. To confirm the network pharmacology results, molecular docking and molecular dynamics simulations were used to verify the binding interactions between the key active ingredients and the key targets.

MATERIALS AND METHODS

Collection of ingredients and targets

A list of ingredients of *Sparganii Rhizoma* was obtained from the Traditional Chinese Medicine Systems Pharmacology Database and Analysis Platform (TCMSP, https://www.tcmsp-e.com/tcmsp.php, Version 2.3), the Bioinformatics Annotation Database for Molecular Mechanism of Traditional Chinese Medicine (BATMAN-TCM database, http://bionet.ncpsb.org.cn/batman-tcm/#/home, Version 2.0) and related literature (Wei *et al.*, 2022; Jia *et al.*, 2021). The chemical structural formula of each ingredient was drawn with ChemDraw software (Version 20.0) and then converted to the InChI format with the Open Babel GUI (Version 2.4.1). Then, the targets of *Sparganii Rhizoma* were screened from the TCMSP and BATMAN-TCM databases based on chemical structural formula.

With the keywords 'lung cancer' and 'lung carcinoma', the related targets of lung cancer in Homo sapiens were retrieved from the DrugBank Online database (https://go.drugbank.com/, version 5.1.13). Then, targets with Z'-scores≥ 22.37 were selected as potential targets for further analysis. Subsequently, the potential targets of *Sparganii Rhizoma* and lung cancer were studied with intersection analysis. The overlapping targets were present in both the pathological processes of lung cancer and the pharmacological effects of Sparganii Rhizoma, so they were identified as potential targets of Sparganii Rhizoma in lung cancer, and the related ingredients of these targets were considered potential active ingredients of Sparganii Rhizoma in lung cancer.

Construction of protein - protein interaction (PPI) network

The targets for *Sparganii Rhizoma* in lung cancer were imported into the STRING database (https://cn.string-db.org/, version 12.0) to investigate PPIs. The minimum required interaction score was set to high confidence, the interaction relationship type was set to Homo sapiens and the remaining parameters were set to default. Then, the PPI network was built using Cytoscape (version 3.9.0). In the network diagram, the node represented the target, and the edge indicated an association between the two targets. The size of each target node was determined by the number of active ingredients related to the target. So, a node with a larger size indicated that the target could activate more active ingredients of Sparganii Rhizoma in lung cancer, and a node with more edges indicated that the target had a more vital position in regulating communication and disseminating information in the PPI network. Based on the above principles, the potential key targets were selected.

GO and KEGG enrichment analysis

To investigate the biological function, Gene Ontology (GO) enrichment and Kyoto Encyclopedia of Genes and Genomes (KEGG) signaling pathway enrichment analyses were retrieved from the Metascape database (https://metascape.org/gp/index.html#/main/, version v3.5.20250701). To uncover the mechanisms, three functional data sets from GO analysis (biological process, cellular component, and molecular function) and KEGG signaling pathway enrichment data were selected, with significant biological annotations set at $p < 0.05$. Afterward, the top 10 GO analysis data and the top 20 KEGG signaling pathway data were used to build diagrams, respectively.

Ingredient - target - pathway network

To clarify the complex relationships among the active ingredients, targets, and pathways for Sparganii Rhizoma in lung cancer, the active ingredients with more than 3 targets, the overlapping targets, and the top 20 KEGG signaling pathways were imported into Cytoscape to construct the ingredient-target-pathway network. In the network diagram, nodes represented ingredients, targets, or pathways, while edges indicated associations between nodes. The number of its related targets determined the size of each ingredient node or pathway node, while the size of each target node was associated with the number of its related active ingredients. The width of the edge between the active ingredient and the target was determined by the value of Z'-score, while the width of the edge between the target and the pathway was associated with the value of enrichment. So, a node with a larger size showed better performance for Sparganii Rhizoma in lung cancer, and an edge with greater width indicated stronger interaction between the two nodes. Based on the above principles, the key potential active ingredients and key targets were selected.

Molecular docking

The three-dimensional protein structures of the key targets were downloaded in PDB format from the RCSB Protein Data Bank (https://www.rcsb.org/). The Discovery Studio software (Version 4.5) was used to remove ligands, ions, waters, and other solvent molecules, and to add hydrogen atoms. Then, the chemical structures of the key active ingredients were converted to the PDB format at their minimum-energy conformations using the ChemBio-UCSF Builder software (Version Ultra 14.0). Next, the AutoDock Tools software (Version 1.5.6) was used to convert the PDB files to the Pdbqt format. Using docking boxes of suitable size that cover the entire target protein, molecular docking was performed with AutoDock Vina (Version 1.1.2). Finally, the visualization was obtained for the target-active ingredient pair at the optimal binding energy. Furthermore, the PyMOL software (Version 1.7.2.1) and the Discovery Studio software were utilized to analyze the binding site, bond length and the types of binding interaction and create the three-dimensional conformation image (Liu *et al.*, 2024; Bisht *et al.*, 2024; Li *et al.*, 2023; Luo *et al.*, 2023; Sun *et al.*, 2023; Dai *et al.*, 2021).

Molecular dynamics simulation

To better understand the interaction between the key active ingredient and the key target, the top three ingredient-target complexes were selected for molecular dynamics simulation. Firstly, the topology file for the key active ingredient was generated using the CHARMM22 force field with the Perl software (version 5.40.2.1), the GROMACS software (version modified 2020.6), and the SwissParam database (https://old.swissparam.ch/). Then, the topology file for the key target was prepared using the CHARMM36 all-atom force field and the CHARMM-modified TIP3P water model in PyMOL and GROMACS. To obtain a good, accurate physiological environment, the simulation was performed in a dodecahedron water box using the SPC216 water model, and the distance between the target protein and the water box's edge was maintained at a minimum of 1.0 nm. Then, the ions were added to neutralize the charge with the default parameters. Subsequently, the energy minimization was optimized with a maximum steep of 50,000 steps and a maximum force of 1000.0 kJ/mol/nm, and the equilibration of temperature and pressure was set for a total duration of 1000 ps. The final molecular dynamics simulation was conducted in 100 ns. At last, the root mean square deviation (RMSD) and root mean square fluctuation (RMSF) were calculated and visualized.

RESULTS

Active ingredients and targets

After exploring chemical ingredients from the TCMSP database, the BATMAN-TCM database, and related literature (Wei et al., 2022; Jia et al., 2021), a total of 129 ingredients were identified for *Sparganii Rhizoma*. Based on the chemical structures, a total of 1101 related targets with 5022 frequencies were identified for these ingredients. The chemical properties, such as molecular formula, Chemical Abstracts Service (CAS) number and number of target gene, were shown in Table S1. After deleting duplicate targets, 150 lung cancer-related targets were retrieved from the DrugBank Online database.

Through the intersection analysis of the targets of Sparganii Rhizoma and lung cancer, 27 overlapping targets were identified as potential targets of Sparganii Rhizoma in lung cancer, and 17 targets with more than 2 active ingredients against lung cancer were shown in Table 1. Then, 57 related ingredients of the overlapping targets were identified as potential active ingredients for Sparganii Rhizoma in lung cancer, and 25 active ingredients with more than two targets were listed in Table 2.

Protein-protein interaction network analysis

The 27 overlapping targets were imported into the STRING database for the PPI network analysis. As shown in Fig. 1, the relationships among the targets were visualized. At the high interaction confidence level, the PPI network consisted of 27 nodes and 37 edges. Using the PPI network parameters calculated by the STRING database and the Cytoscape software, the average node degree was 2.74, the average local clustering coefficient was 0.617, the expected number of edges was 5, and the PPI enrichment p-value was less than 1.0e-16. In the PPI network, the size of each target node was determined by the number of active ingredients. So, the nodes with bigger size, such as Prostaglandin G/H synthase 1 (PTGS1), PTGS2, Cytochrome P450 2E1 (CYP2E1), Fibroblast growth factor receptor 2 (FGFR2) and Liver carboxylesterase 1 (CES1), were identified. Furthermore, the edges indicated the association between the two targets, so targets with more edges, such as Cytochrome P450 3A4 (CYP3A4), CYP2E1, UDP-glucuronosyltransferase 1-1 (UGT1A1), CES1, Cytochrome P450 1A2 (CYP1A2), and PTGS2, would play a more important role in the PPI network. Based on the two principles above, PTGS2, CYP2E1, PTGS1, and CYP1A2 may be key targets of Sparganii Rhizoma in lung cancer.

GO enrichment analysis

The three GO enrichment analysis functions were performed using 27 overlapping targets in the Metascape database. As listed in table S2, there were 543 terms of biological processes, 90 terms of molecular functions and 24 terms of cellular components. As shown in fig. 2, the top 10 most significant enrichment analysis terms in each functional category were selected.

The results of Fig. 2 showed the targets for biological processes were mainly enriched in response to xenobiotic stimulus, cellular response to xenobiotic stimulus, xenobiotic metabolic process, xenobiotic transport, xenobiotic transmembrane transport, response to toxic substance, steroid metabolic process, small molecule biosynthetic process, reactive oxygen species metabolic process and response to oxidative stress. The top 10 terms of enriched molecular functions included heme binding, tetrapyrrole binding, oxidoreductase activity, aromatase activity, oxidoreductase activity - acting on paired donors, antioxidant activity, uridine transmembrane transporter activity, pyrimidine nucleobase transmembrane transporter activity, pyrimidine nucleoside transmembrane transporter activity and oxidoreductase activity - with incorporation of one atom of oxygen. The top 10 cellular components were associated with the apical plasma membrane, the apical part of the cell, the intercellular canaliculus, the neuronal cell body, the cell body, the nuclear envelope, the receptor complex, the basolateral plasma membrane, the basal plasma membrane, and the basal part of the cell. Furthermore, two important GO enrichment terms were identified, as shown in table S2, namely lung development and lung morphogenesis. The targets enriched in lung development included CYP1A2, FGFR2, and MAP2K1, while lung morphogenesis was associated with FGFR2 and MAP2K1. So, these targets may be key targets in the GO function for Sparganii Rhizoma in lung cancer.

Table 1: The target information of *Sparganii Rhizoma* on lung cancer.

Target	Target gene	Uniprot ID	Number of ingredients
Prostaglandin G/H synthase 1	PTGS1	P23219	13
Prostaglandin G/H synthase 2	PTGS2	P35354	13
Cytochrome P450 2E1	CYP2E1	P05181	12
Fibroblast growth factor receptor 2	FGFR2	P21802	10
Liver carboxylesterase 1	CES1	P23141	8
Cytochrome P450 1A2	CYP1A2	P05177	5
UDP-glucuronosyltransferase 1-1	UGT1A1	P22309	5
Cytochrome P450 19A1	CYP19A1	P11511	3
Cytochrome P450 3A4	CYP3A4	P08684	3
NAD(P)H dehydrogenase [quinone] 1	NQO1	P15559	3
Solute carrier family 28 member 3	SLC28A3	Q9HAS3	3
Equilibrative nucleoside transporter 1	SLC29A1	Q99808	3
Equilibrative nucleoside transporter 2	SLC29A2	Q14542	3
DNA topoisomerase 1	TOP1	P11387	3
Canalicular multispecific organic anion transporter 1	ABCC2	Q92887	2
Dual specificity mitogen-activated protein kinase kinase 1	MAP2K1	Q02750	2
Myeloperoxidase	MPO	P05164	2
Proto-oncogene tyrosine-protein kinase receptor Ret	RET	P07949	2

Table 2: The information of active ingredients from Sparganii Rhizoma on lung cancer.

Ingredients	CAS No.	Molecular formula	Number of targets
adenosine	58-61-7	C10H13N5O4	6
docosanoic acid	112-85-6	C22H44O2	4
linoleic acid	60-33-3	C18H32O2	4
lauric acid	143-07-7	C12H24O2	4
1-hexanoic acid	142-62-1	C6H12O2	4
octadecan-1-ol	8034-90-0	C18H38O	3
hexadecan-1-ol	36653-82-4	C16H34O	3
1-hydroxy-2-acetyl-4-methylbenzene	1450-72-2	C9H10O2	3
4-hydroxybenzoic acid	99-96-7	C7H6O3	3
4-hydroxycinnamic acid	7400-08-0	C9H8O3	3
betulinic acid	472-15-1	C30H48O3	3
lily aldehyde	80-54-6	C14H20O	3
methyl linoleate	112-63-0	C19H34O2	3
ethyl linoleate	544-35-4	C20H36O2	3
1-octanol	111-87-5	C8H18O	3
(7E)-6,9,10-trihydroxy-7-octadecenoic acid	/	C18H34O5	2
2-acetyl pyrrole	1072-83-9	C6H7NO	2
9(S),12(S),13(S)-trihydroxy-10(E)-octadecenoic acid	/	C18H34O5	2
cyclo(Tyr-Leu)	82863-65-8	C15H20N2O3	2
butyric Acid	107-92-6	C4H8O2	2
4-hydroxybenzaldehyde	123-08-0	C7H6O2	2
phenanthrene-9,10-dione	84-11-7	C14H8O2	2
succinic acid	110-15-6	C4H6O4	2
dehydrocostus lactone	477-43-0	C15H18O2	2
sparstolonin B	1259330-61-4	C15H8O5	2

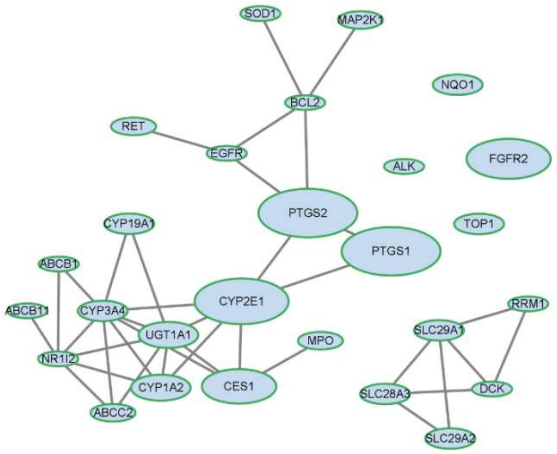

Fig. 1: Protein-protein interaction (PPI) network of targets for Sparganii Rhizoma on lung cancer.

KEGG signaling pathway enrichment analysis

The KEGG signaling pathway enrichment analysis was performed with 27 overlapping targets in the Metascape database. As listed in table S2, there were 86 terms of KEGG signaling pathways. As shown in fig. 3, the top 20 significantly enriched KEGG signaling pathways were selected. In fig. 3, the horizontal axis showed the enrichment values, the circle size indicated the number of related targets in the pathway and the circle color indicated the significance value.

As shown in fig. 3, the KEGG signaling pathways enriched in cancer were including chemical carcinogenesis - DNA adducts, pathways in cancer, chemical carcinogenesis - receptor activation, chemical carcinogenesis - reactive oxygen species, gastric cancer, central carbon metabolism in cancer, non-small cell lung cancer, prostate cancer, microRNAs in cancer and the mainly targets enriched in these pathways were including MAP2K1, FGFR2, PTGS2 and so on. Especially, there were two vital KEGG signaling pathways: non-small cell lung cancer (as shown in Fig. 3) and small cell lung cancer (as listed in Table S2). The targets enriched in non-small cell lung cancer included MAP2K1, Proto-oncogene tyrosine-protein kinase receptor Ret (RET) and others, whereas small cell lung cancer was associated with PTGS2. So, these targets may be key targets in the KEGG signaling pathways for Sparganii Rhizoma in lung cancer.

Ingredient - target - pathway network analysis

To explore the molecular mechanism of *Sparganii Rhizoma* in lung cancer, an ingredient-target-pathway network was constructed. As shown in fig. 4, 15 active ingredients with more than 3 targets were associated with 26 targets, and the top 20 significant enrichment KEGG signaling pathways were identified. The ingredient-target-pathway network illustrated the mechanisms underlying multiple ingredients, targets, and pathways of Sparganii Rhizoma in lung cancer.

In the network diagram of fig. 4, a node with a larger size indicates that it had more ingredients for the target, or more targets for the ingredient and pathway. In contrast, a wider edge indicates a stronger interaction between the nodes. Integrated the results of the PPI network (Fig. 1), GO enrichment analysis (Fig. 2), KEGG signaling pathway enrichment analysis with the ingredient-target-pathway network (Fig. 4), the targets, including PTGS2, PTGS1, MAP2K1, CYP1A2, CYP2E1, FGFR2 and CES1, were presented as the potential key targets for *Sparganii Rhizoma* on lung cancer. The ingredients associated with these potential key targets, such as adenosine, sparstolonin B, emodin, 4-hydroxycinnamic acid, docosanoic acid, linoleic acid, lauric acid, and 1-hexanoic acid, were considered key active ingredients of Sparganii Rhizoma in lung cancer. The above potential key active ingredients and key targets will be confirmed through subsequent molecular docking and molecular dynamics simulations.

Molecular docking verification

Molecular docking is an important method in structural molecular biology. Based on the network pharmacology results, the key potential active ingredients and targets were studied using molecular docking. It is generally recognized that the target and the ingredient with lower binding energy would have a stronger affinity and a more stable molecular model. Docking affinities below -5.0 kcal/mol indicated good binding between the target and the ingredient, and affinities below -7.0 kcal/mol indicated a strong binding model (Liu *et al.*, 2024; Ye *et al.*, 2021). As summarized in the table 3, the targets were ranked according to the docking affinity: CYP1A2 (-7.5 ± 2.3 kcal/mol) > PTGS2 (-6.9 ± 1.8 kcal/mol) > MAP2K1 (-6.7 ± 2.0 kcal/mol) > FGFR2 (-6.4 ± 1.7 kcal/mol) > PTGS1 (-6.0 ± 2.1 kcal/mol) > CYP2E1 (-5.9 ± 1.7 kcal/mol) > CES1 (-5.8 ± 1.6 kcal/mol), so these targets had good binding performance. For the active ingredients, the sequence was as follows: sparstolonin B (-9.3 ± 1.0 kcal/mol) > emodin (-9.1 ± 1.0 kcal/mol) > adenosine (-6.8 ± 1.0 kcal/mol) > 4-hydroxycinnamic acid (-6.4 ± 0.6 kcal/mol) > linoleic acid (-5.2 ± 1.1 kcal/mol) > lauric acid (-5.0 ± 1.0 kcal/mol) > docosanoic acid (-4.9 ± 0.4 kcal/mol) > 1-hexanoic acid (-4.8 ± 0.4 kcal/mol), so sparstolonin B, emodin, adenosine, 4-hydroxycinnamic acid, linoleic acid and lauric acid had good binding performance. Notably, sparstolonin B and emodin exhibited the strongest binding affinity for all key targets. As shown in fig. 5, the complex with the lowest docking affinity was visualized in the three-dimensional interaction model for each key target. The lowest docking affinity was the complex of CYP1A2 and sparstolonin B (docking affinity: -11.1 kcal/mol) and the main intermolecular forces involved van der Waals forces of Isoleucine (ILE) - A117 (located at position 117 on protein chain A), Threonine (THR) - A118, Asparagine (ASN) - A312, etc, carbon-hydrogen bonds with Aspartic acid (ASP) - A313 (bond length: 3.71 Å) and so on.

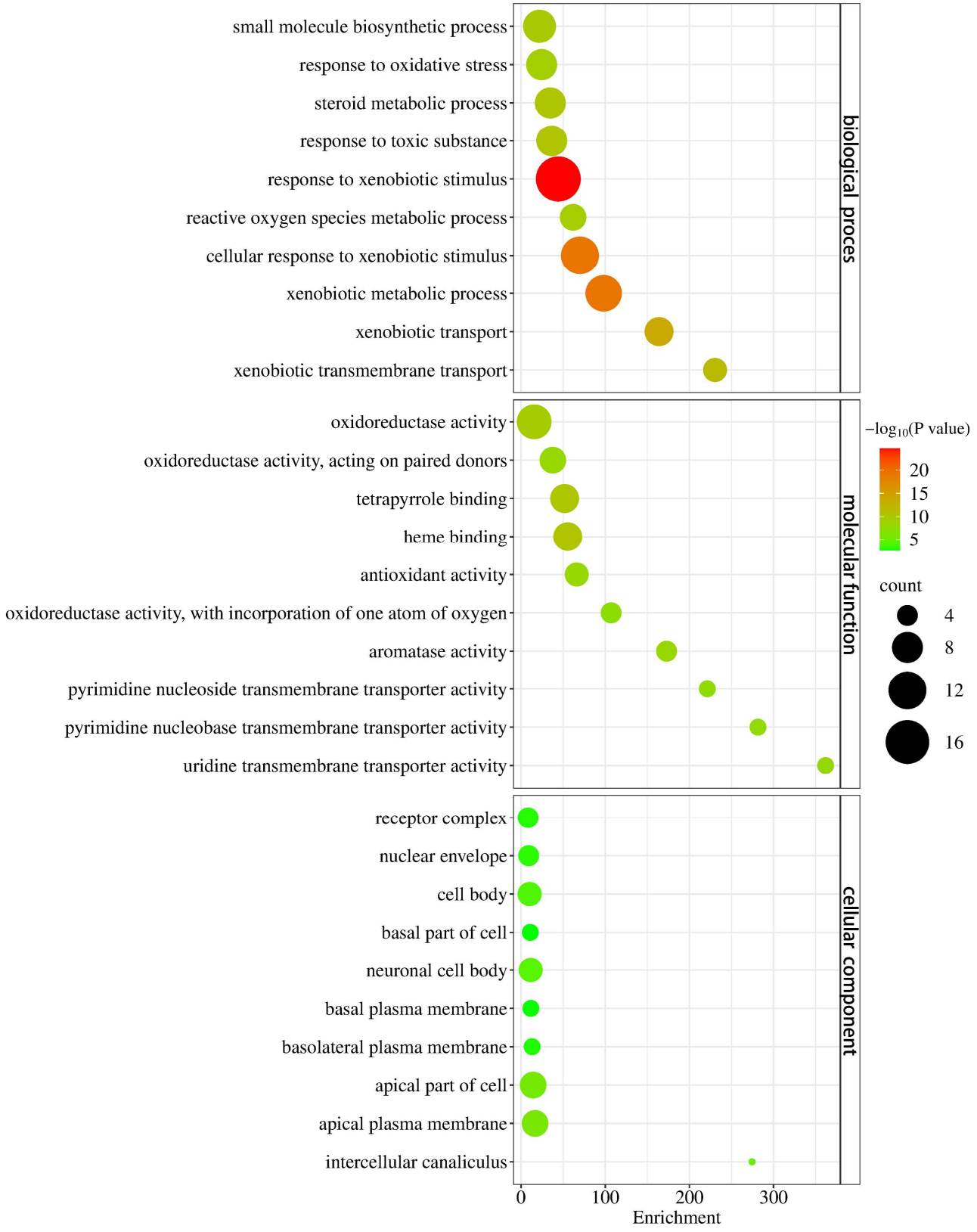

Fig. 2: The biological process, molecular function and cellular component of Gene Ontology (GO) enrichment analysis.

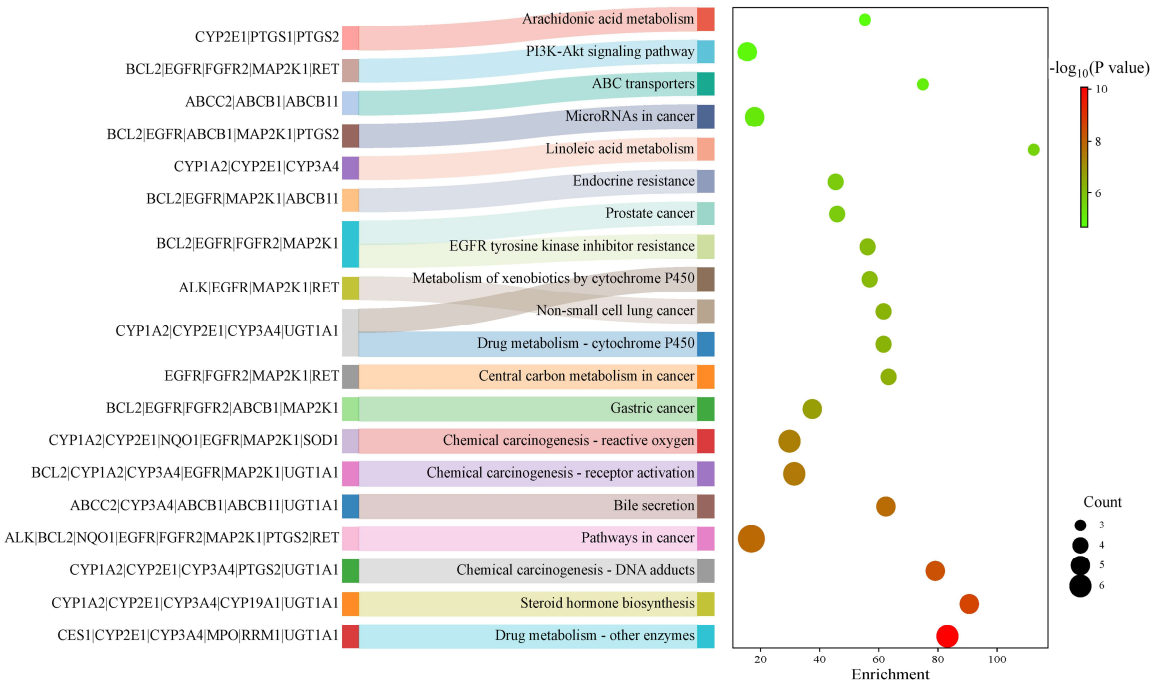

Fig. 3: The Kyoto Encyclopedia of Genes and Genomes (KEGG) signaling pathway enrichment analysis of the targets.

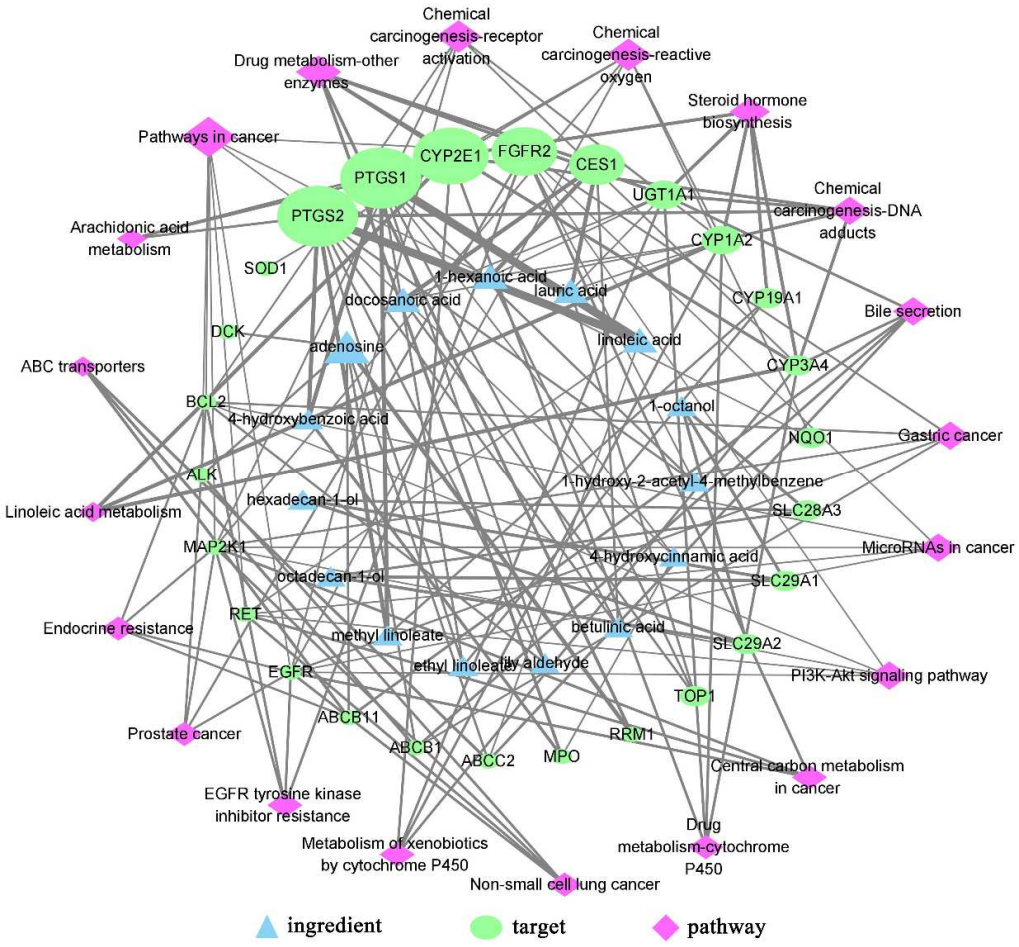

Fig. 4: The ingredient - target - pathway network of Sparganii Rhizoma on lung cancer.

Table 3: Molecule docking affinity (kcal/mol) of the potential key active ingredients and key targets.

	PTGS1	PTGS2	CYP2E1	FGFR2	CYP1A2	CES1	MAP2K1
adenosine	-6.3	-6.9	-5.9	-6.1	-7.1	-6.4	-8.9
docosanoic acid	-4.6	-5.3	-4.3	-5.1	-5.0	-5.0	-5.2
linoleic acid	-4.1	-5.8	-3.7	-6.0	-6.8	-4.7	-5.4
lauric acid	-3.8	-5.7	-5.4	-5.3	-6.3	-4.0	-4.6
1-hexanoic acid	-4.6	-5.1	-4.8	-4.5	-5.5	-4.4	-4.9
sparstolonin B	-9.2	-9.7	-8.4	-9.0	-11.1	-7.9	-9.5
4-hydroxycinnamic acid	-6.4	-6.7	-6.2	-6.1	-7.5	-5.4	-6.2
emodin	-8.7	-9.6	-8.1	-9.0	-11.0	-8.2	-8.9

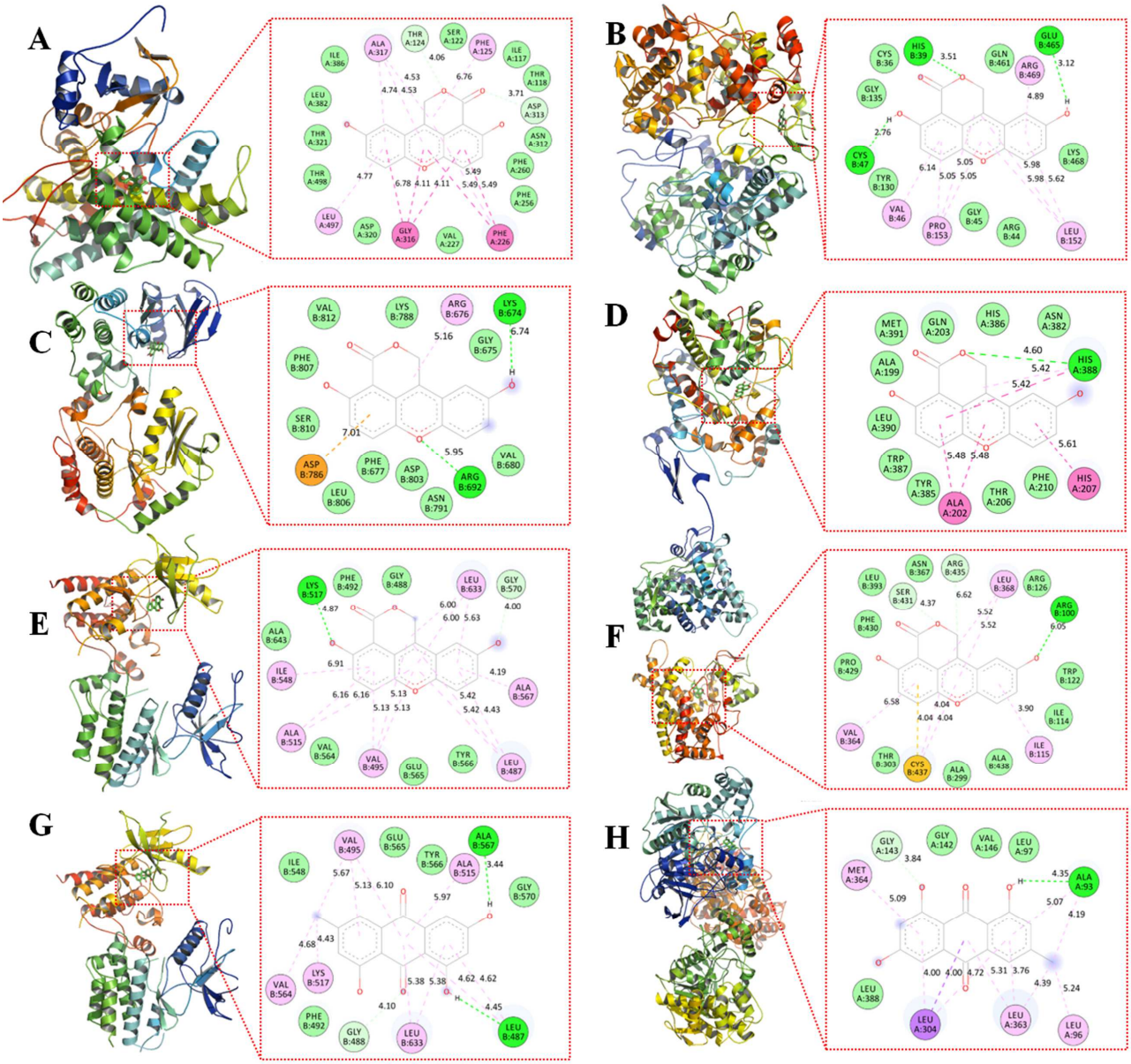

Fig. 5: Molecular docking results of (A) CYP1A2; (B) PTGS2; (C) MAP2K1; (D) PTGS1; (E) FGFR2 and; (F) CYP2E1 with sparstolonin B; (G) FGFR2 and; (H) CES1 with emodin.

The followed was the complex of PTGS2 and parstolonin B (docking affinity: -9.7 kcal/mol) and the main forces included conventional hydrogen bond with Cysteine (CYS) - B47 (bond length: 2.76 Å), Glutamic acid (GLU) - B465 (bond length: 3.12 Å) and Histidine (HIS) - A39 (bond length: 3.51 Å) and van der Waals forces with CYS - B36, Lysine (LYS) - B468, Glycine (GLY) - B45, etc.

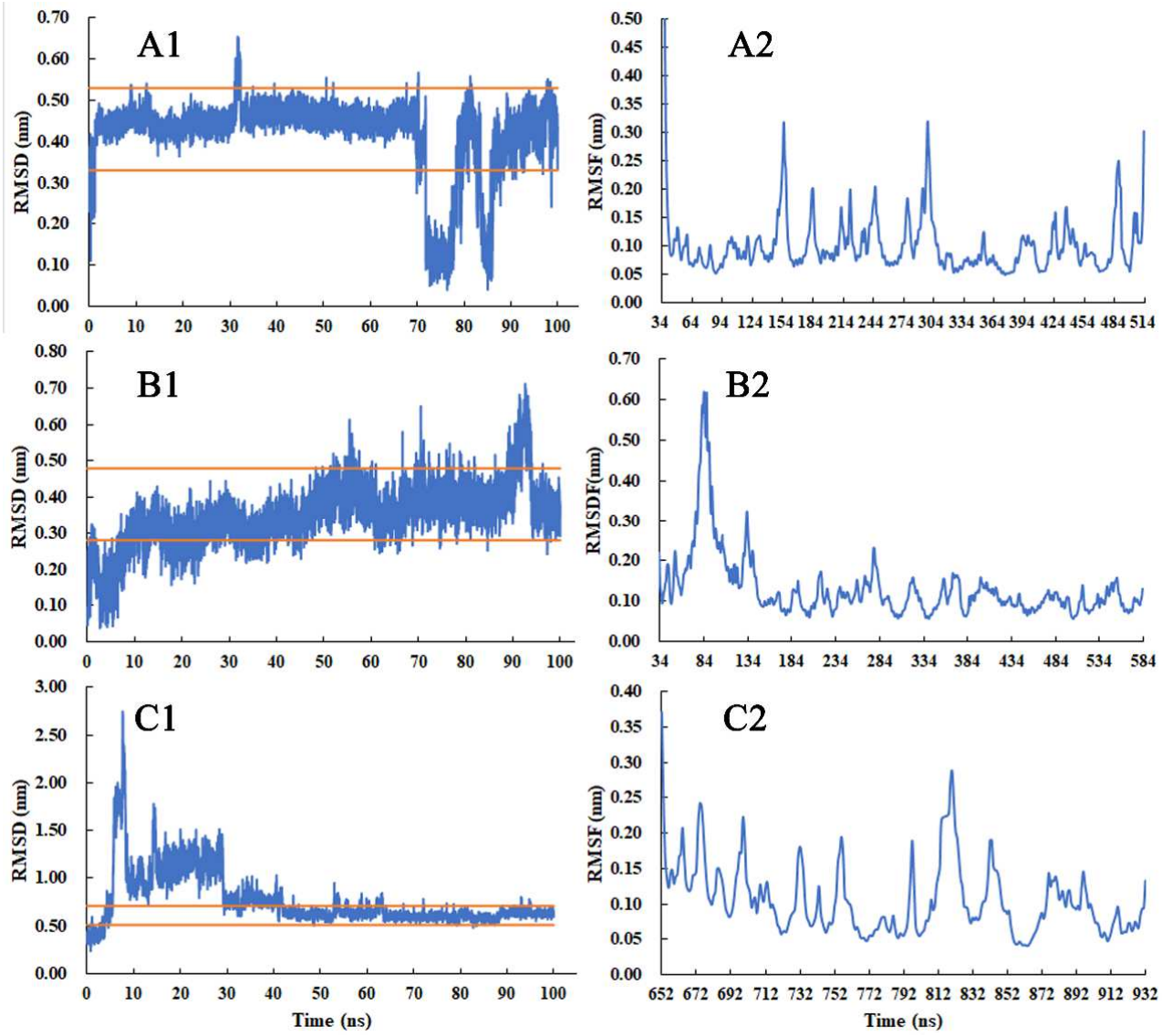

Fig. 6: Result of molecular dynamics simulation for (A) CYP1A2, (B) PTGS2 and (C) MAP2K1 with sparstolonin B (1 - RMSD, Root Mean Square Deviation; 2 - RMSF, Root Mean Square Fluctuation).

The third was MAP2K1 - sparstolonin B (docking affinity: -9.5 kcal/mol). Furthermore, the top three complexes with the lowest docking affinity would be studied using molecular dynamics simulation.

Verification of molecular dynamics simulation

In molecular dynamics simulations, two important parameters are the root-mean-square deviation (RMSD) and the root-mean-square fluctuation (RMSF) (Bisht *et al.*, 2024; Liu *et al.*, 2024; Sun *et al.*, 2023). RMSD measures the average deviation of the structure from its initial state in the simulation, so it can reflect the stability and dynamic properties across different conformations. Generally, RMSD differences of less than 0.2 nm are considered indicative of a stable conformation. RMSF is used to quantify fluctuations in amino acid residues during the simulation. A higher value of RMSF means the corresponding protein region is more flexible, so this region may be the active site, or located in the active pocket of the protein (Bisht *et al.*, 2024; Sun *et al.*, 2023; Luo *et al.*, 2023; Ye *et al.*, 2021; Liu *et al.*, 2024; Li *et al.*, 2023).

Based on molecular docking results, the top three complexes with the lowest docking affinities were selected for molecular dynamics simulation. As shown in fig. 6, the RMSD for the complex of MAP2K1 and sparstolonin B fluctuated in the early stage (0 - 40 ns), then stabilized at a value less than 0.2 nm. For the RMSD of CYP1A2-sparstolonin B and PTGS2-sparstolonin B, there were short-term fluctuations in the middle stage, and they remained stable for most of the time period. The conformations of the three complexes above were stable. The RMSF curve in fig. 6 showed fluctuations in the amino acid residues. For the complex of CYP1A2 and

sparstolonin B, there were three big fluctuation excluding the head and tail regions of the protein chain. For PTGS2 - sparstolonin B, there was a region (amino acid residues 74-94) that had significantly greater flexibility than other regions. The MAP2K1-sparstolonin B complex also exhibited many flexible regions. The results of the molecular dynamics simulation showed that CYP1A2, PTGS2, and MAP2K1 had multiple active regions and could bind stably to sparstolonin B.

DISCUSSION

As a famous anti-cancer herb, the active ingredients and mechanism of *Sparganii Rhizoma* for lung cancer are not yet clear. Based on the integration of network pharmacology, molecular docking, and molecular dynamics simulation, this study aimed to identify potential active ingredients and the mechanism of Sparganii Rhizoma in lung cancer.

In this study, 57 potential active ingredients were identified for *Sparganii Rhizoma* on lung cancer and sparstolonin B and emodin were confirmed as two key active ingredients. Sparstolonin B is a compound of oxygen-mixed anthracene with the chemical structure of polyphenol, xanthone and isocoumarin. Qinghe Meng *et al*. reported that a nanoformulation of Sparstolonin B could reduce levels of several inflammatory factors through the MyD88/NF-κB signaling pathways in mouse lung injury and in RAW264.7 cells (Meng *et al.*, 2025). It has previously been found that sparstolonin B significantly decreased cell viability in both human breast cancer and ovarian epithelial cancer cell lines, without causing toxicity in human fibroblasts (Dilber *et al.*, 2024). Shaozhuang Liu *et al*. discovered that sparstolonin B could inhibit the proliferation and migration and induce apoptosis in prostate cancer cells and in nude mouse xenograft models (Liu *et al.*, 2021). Emodin is a natural anthraquinone compound with diverse pharmacological effects. It has previously screened 330 small molecules for breast cancer and found that emodin could block the transcription of vascular endothelial growth factor A during zebrafish vascular development and in tumor angiogenesis in breast cancer-bearing mice (Zou *et al.*, 2020). Zhennv Shen *et al*. discovered that emodin could inhibit proliferation and induce apoptosis in colorectal cancer cells (Shen *et al.*, 2024).

A total of 27 targets were identified by network pharmacology for *Sparganii Rhizoma* in lung cancer, and CYP1A2, PTGS2, and MAP2K1 were verified as the three key targets by molecular docking and molecular dynamics simulation. CYP1A2 is an important inducible CYP protein in the human liver and a key enzyme in the activation of major lung carcinogens and lung inflammation (Pavanello *et al.*, 2012). A prospective study of 425 lung cancer cases investigated the interactions of three CYP1A2 functional polymorphisms, analyzed the relationship between CYP1A2 genetic polymorphisms and the risk of lung cancer, and found that CYP1A2 could influence the development of lung cancer through lung carcinogen activation, lung inflammation, and so on (Pavanello *et al.*, 2012). PTGS2, also known as Cyclooxygenase-2, is often overexpressed in various cancers, including lung cancer. As an important inflammation factor, the upregulation of PTGS2 would enhance a number of tumorigenic events in lung cancer, such as promoting tumor proliferation and invasion, promoting angiogenesis, decreasing host immunity, and increasing resistance to apoptosis (Liu *et al.*, 2015). Yexuan Lin *et al*. reported a PTGS2-targeted oligonucleotide drug, HQi-sRNA-2, derived from the well-known traditional Chinese medicine Huangqin, which could significantly inhibit proliferation, migration, and invasion, and induce apoptosis in lung cancer cells (Lin *et al.*, 2024). A hospital-based case-control study (684 lung cancer patients and 604 controls) revealed an association between two extensively studied PTGS2 polymorphisms (rs689466 and rs5275) and lung cancer risk in northeastern Chinese (Guo *et al.*, 2012). MAP2K1 is part of the Ras signaling pathway and a convergence point for multiple kinases and intracellular signals in the Rapidly Accelerated Fibrosarcoma signaling, so MAP2K1 plays an important role in transcriptional regulation, regulating cell proliferation and differentiation in lung cancer (Scheffler *et al.*, 2020). Jiacong You *et al*. reported that miR-449a, by inhibiting MAP2K1 expression, reduced cell invasion in non-small cell lung cancer in both *in vitro* and *in vivo* settings (You *et al.*, 2015).

CONCLUSION

With a high cancer incidence rate and mortality rate, lung cancer has brought a huge disease burden to patients' families and society. As a famous anti-cancer herb for years, the underlying active ingredients and mechanism of *Sparganii Rhizoma* on lung cancer have not yet been clear. Based on the integration of network pharmacology, molecular docking, and molecular dynamics simulation, this study aimed to reveal the potential active ingredients and mechanism of Sparganii Rhizoma in lung cancer. Network pharmacology identified 57 active ingredients, 27 targets and 86 KEGG signaling pathways. Molecular docking and molecular dynamics simulations showed that the key active ingredients were sparstolonin B and emodin, and the key targets were CYP1A2, PTGS2 and MAP2K1. This study provided a solid foundation for further research on Sparganii Rhizoma and lung cancer, and also offered a promising method and valuable insights for future research on traditional herbs.

Acknowledgements
None.

Authors' contributions
Chang Wei: Conceptualization; Chang Wei, Niu Bingxuan, Yan Xuxu, Hu Chenyang: Data curation, formal analysis

and investigation; Chang Wei and Yan Xuxu: Writing – original draft; Chang Wei: Writing – review and editing.

Funding
This work was supported by Xinxiang Key Laboratory for Precision Therapeutics of Small Cell Lung Cancer (Project No: ZDSYS-213).

Data availability statement
The original data generated or analyzed during this study are included in this published article and its supplementary material. Further inquiries would be available from the corresponding author.

Ethical approval
Not applicable.

Conflict of interest
The authors declare no conflict of interest.

Supplementary data
https://www.pjps.pk/uploads/2026/06/SUP1781005781.pdf

REFERENCES

Bisht A, Tewari D, Kumar S and Chandra S (2024). Network pharmacology, molecular docking and molecular dynamics simulation to elucidate the mechanism of anti-aging action of *Tinospora cordifolia*. *Mol. Divers.,* **28**(3): 1743-1763.

Cao A, He H, Jing M, Yu B and Zhou X (2017). Shenfu injection adjunct with platinum-based chemotherapy for the treatment of advanced non-small-cell lung cancer: A meta-analysis and systematic review. *Evid. Based Compl. Alt. Med.,* **2017**: 1068751.

Chang YL, Xu GL, Wang XP, Yan X, Xu X, Li X, Chen ZK, Ren X, Chen XQ, Zhang JH, Wang XH, Ren XY, Liu XY, Wang Y, Sun SQ, Li X and She GM (2020). Anti-tumor activity and linear-diarylheptanoids of herbal couple *Curcumae Rhizoma-Sparganii Rhizoma* and the single herbs. *J. Ethnopharmacol.,* **250**: 112465.

Dai S, Zhang G, Zhao F and Shu Q (2021). Study on the molecular mechanism of the herbal couple *Sparganii Rhizoma-Curcumae Rhizoma* in the treatment of lung cancer based on network pharmacology. *Evid. Based Compl. Alt.Med.,* **2021**: 6664489.

Detterbeck FC, Woodard GA, Bader AS, Dacic S, Grant MJ, Park HS and Tanoue LT (2024). The proposed ninth edition TNM classification of lung cancer. *Chest,* **166**(4): 882-895.

Dilber Y, Ceker HT, Oztuzun A, Circirli B, Kirimlioglu E, Barut Z and Aslan M (2024). Sparstolonin B reduces estrogen-dependent proliferation in cancer cells: Possible role of ceramide and PI3K/AKT/mTOR inhibition. *Pharmaceuticals,* **17**(12): 1564.

Filho AM, Laversanne M, Ferlay J, Colombet M, Piñeros M, Znaor A, Parkin DM, Soerjomataram I and Bray F (2025). The GLOBOCAN 2022 cancer estimates: Data sources, methods and a snapshot of the cancer burden worldwide. *Int. J. Cancer,* **156**(7): 1336-1346.

Guo S, Li X, Gao M, Kong H, Li Y, Gu M, Dong X and Niu W (2012). Synergistic association of PTGS2 and CYP2E1 genetic polymorphisms with lung cancer risk in northeastern Chinese. *Plos One,* **7**(6): e39814.

Jia J, Li X, Ren X, Liu X, Wang Y, Dong Y, Wang X, Sun S, Xu X, Li X, Song R, Ma J, Yu A, Fan Q, Wei J, Yan X, Wang X and She G (2021). *Sparganii Rhizoma*: A review of traditional clinical application, processing, phytochemistry, pharmacology and toxicity. *J. Ethnopharmacol.,* **268**: 113571.

Jiang Y, Liu LS, Shen LP, Han ZF, Jian H, Liu JX, Xu L, Li HG, Tian JH and Mao ZJ (2016). Traditional Chinese medicine treatment as maintenance therapy in advanced non-small-cell lung cancer: A randomized controlled trial. *Complement. Ther. Med.,* **24**: 55-62.

Lee E and Kazerooni EA (2022). Seminars in respiratory and critical care medicine. *Semin. Respi.r Crit. Care. Med.,* **43**(6): 839-850.

Li X, Miao F, Xin R, Tai Z, Pan H, Huang H, Yu J, Chen Z and Zhu Q (2023). Combining network pharmacology, molecular docking, molecular dynamics simulation and experimental verification to examine the efficacy and immunoregulation mechanism of FHB granules on vitiligo. *Front. Immunol.,* **14**: 1194823.

Lin Y, Sun N, Liu D, Yang X, Dong Y and Jiang C (2024). COX-2/PTGS2-targeted herbal-derived oligonucleotide drug HQi-sRNA-2 was effective in spontaneous mouse lung cancer model. *IUBMB Life,* **76**(11): 937-950.

Liu J, Gao D, Ding Q, Zhang B, Zhu W and Shi Y (2023). Sparganii Rhizoma alleviates pulmonary fibrosis by inhibiting fibroblasts differentiation and epithelial-mesenchymal transition mediated by TGF-β1/ Smad2/3 pathway. *J. Ethnopharmacol.,* **309**: 116305.

Liu M, Wang Y, Deng W, Xie J, He Y, Wang L, Zhang J and Cui M (2024). Combining network pharmacology, machine learning, molecular docking and molecular dynamic to explore the mechanism of Chufeng Qingpi decoction in treating schistosomiasis. *Front. Cell. Infect. Microbiol.,* **14**: 1453529.

Liu R, Xu KP and Tan GS (2015). Cyclooxygenase-2 inhibitors in lung cancer treatment: Bench to bed. *Eur. J. Pharmacol.,* **769**: 127-133.

Liu S, Hu J, Shi C, Sun L, Yan W and Song Y (2021). Sparstolonin B exerts beneficial effects on prostate cancer by acting on the reactive oxygen species-mediated PI3K/AKT pathway. *J. Cell. Mol. Med.,* **25**(12): 5511-5524.

Luo W, Deng J, He J, Yin L, You R, Zhang L, Shen J, Han Z, Xie F, He J and Guan Y (2023). Integration of

molecular docking, molecular dynamics and network pharmacology to explore the multi-target pharmacology of fenugreek against diabetes. *J. Cell. Mol. Med.,* **27**(14): 1959-1974.

Meng Q, Wang X, Guo D, Zhang G, Shi C, Novak A, Yang X, Luo J and Cooney RN (2025). Sparstolonin B nano-formulation attenuates LPS-induced lung injury. *Front. Pharmacol.,* **16**: 1532391.

Nooreldeen R and Bach H (2021). Current and future development in lung cancer diagnosis. *Int. J. Mol. Sci.,* **22**(16): 8661.

Pavanello S, Fedeli U, Mastrangelo G, Rota F, Overvad K, Raaschou-Nielsen O, Tjønneland A and Vogel U (2012). Role of CYP1A2 polymorphisms on lung cancer risk in a prospective study. *Cancer Genet,* **205**(6): 278-284.

Scheffler M, Holzem A, Kron A, Nogova L, Ihle MA, von Levetzow C, Fassunke J, Wompner C, Bitter E, Koleczko S, Abdulla DSY, Michels S, Fischer R, Riedel R, Weber JP, Westphal T, Gerigk U, Kern J, Kaminsky B, Randerath W, Kambartel KO, Merkelbach-Bruse S, Büttner R and Wolf J (2020). Co-occurrence of targetable mutations in Non-small cell lung cancer (NSCLC) patients harboring MAP2K1 mutations. *Lung Cancer,* **144**: 40-48.

Shen M, Wang YJ, Liu ZH, Chen YW, Liang QK, Li Y and Ming HX (2023). Inhibitory effect of astragalus polysaccharide on premetastatic niche of lung cancer through the S1PR1-STAT3 signaling pathway. *Evid. Based. Compl. Alt. Med.,* **2023**: 4010797.

Shen Z, Zhao L, Yoo SA, Lin Z, Zhang Y, Yang W and Piao J (2024). Emodin induces ferroptosis in colorectal cancer through NCOA4-mediated ferritinophagy and NF-κb pathway inactivation. *Apoptosis,* **29**(9-10): 1810-1823.

Sun Z, Wang Y, Pang X, Wang X and Zeng H (2023). Mechanisms of polydatin against spinal cord ischemia-reperfusion injury based on network pharmacology, molecular docking and molecular dynamics simulation. *Bioorg. Chem.,* **140**: 106840.

Thai AA, Solomon BJ, Sequist LV, Gainor JF and Heist RS (2021). Lung cancer. *Lancet,* **398**(10299): 535-554.

Wei J, Wang X, Dong Y, Zhong X, Ren X, Song R, Ma J, Yu A, Fan Q, Yao J, Shan D, Lv F, Zheng Y, Deng Q, Li X, He Y, Fan S, Zhao C, Wang X, Yuan R and She G (2022). Curcumae Rhizoma - combined with Sparganii Rhizoma in the treatment of liver cancer: Chemical analysis using UPLC-LTQ-Orbitrap MS(n), network analysis and experimental assessment. *Front. Pharmacol.,* **13**: 1027687.

Xi Z, Dai R, Ze Y, Jiang X, Liu M and Xu H (2025). Traditional Chinese medicine in lung cancer treatment. *Mol. Cancer,* **24**(1): 57.

Ye J, Li L and Hu Z (2021). Exploring the molecular mechanism of action of Yinchen Wuling powder for the treatment of hyperlipidemia, using network pharmacology, molecular docking and molecular dynamics simulation. *Biomed. Res. Int.,* **2021**: 9965906.

You J, Zhang Y, Li Y, Fang N, Liu B, Zu L and Zhou Q (2015). MiR-449a suppresses cell invasion by inhibiting MAP2K1 in non-small cell lung cancer. *Am. J. Cancer Res.*, **5**(9): 2730-2744.

Zhang P, Zhang D, Zhou W, Wang L, Wang B, Zhang T and Li S (2024). Network pharmacology: Towards the artificial intelligence-based precision traditional Chinese medicine. *Brief Bioinform.,* **25**(1): 1-12.

Zhao L, Zhang H, Li N, Chen J, Xu H, Wang Y and Liang Q (2023). Network pharmacology, a promising approach to reveal the pharmacology mechanism of Chinese medicine formula. *J. Ethnopharmacol.,* **309**: 116306.

Zheng M, Zhang R, Yang X, Wang F, Guo X, Li L, Wang J, Shi Y, Miao S, Quan W, Ma S and Shi X (2025). Integrating network pharmacology, molecular docking and bioinformatics to explore the mechanism of *Sparganii Rhizoma* in the treatment of laryngeal cancer. *Mol. Divers.*, **29**(6): 6325-6342.

Zhou W, Zhang H, Wang X, Kang J, Guo W, Zhou L, Liu H, Wang M, Jia R, Du X, Wang W, Zhang B and Li S (2022). Network pharmacology to unveil the mechanism of Moluodan in the treatment of chronic atrophic gastritis. *Phytomedicine,* **95**: 153837.

Zou G, Zhang X, Wang L, Li X, Xie T, Zhao J, Yan J, Wang L, Ye H, Jiao S, Xiang R and Shi Y (2020). Herb-sourced emodin inhibits angiogenesis of breast cancer by targeting VEGFA transcription. *Theranostics,* **10**(15): 6839-6853.